INTERNATIONAL JOURNAL OF PRECISION ENGINEERING AND MANUFACTURING Vol. 17, No. 1, pp. 109-117 JANUARY 2016 / 109
DOI: 10.1007/s12541-016-0014-z ISSN 2234-7593 (Print) / ISSN 2005-4602 (Online)

Simulation and Experiments on the Drying Outcome of Drying Drums

Sijia Chen[1] and Jianhong Yang[1,#]

1 College of Mechanical Engineering and Automation, Huaqiao University, Xiamen, 361-021, China
Corresponding Author / E-mail: yjhong@hqu.edu.cn, TEL: +86-18959291108, FAX: +86-592-6162588

KEYWORDS: Discrete element method, Drying drums, Numerical simulation, Particle motion, Temperature distribution

In order to research the drying efficiency of a rotary dryer, a three-dimensional simulation model of roller is built. The temperature distribution in the dryer is simulation modeled using Fluent code, and the simulation result is contrastively analyzed by a thermal imaging test. Using the material curtain distribution location and uniformity as evaluation parameters, EDEM studies the impact of the dryer's internal structural parameters and the production parameters on the material curtain distribution characteristics. A contrast experiment is conducted to obtain the optimized structural parameters and production parameters of a rotary dryer.

Manuscript received: June 24, 2015 / Revised: September 26, 2015 / Accepted: October 18, 2015

NOMENCLATURE

G_1 = yield of the drying drum
C_1 = moisture content of dry basis of initial material
C_2 = moisture content of dry basis of product
W_1 = water content of initial material
W_2 = water content of product
G_c = amount of dry material
G_0 = feed rate of sands
W = rate of evaporation
Q_1 = heat quantity of evaporating water in wet material
Q_2 = heat quantity of heating up material
Q_3 = thermal energy loss through system
Q = total heat required
q = latent heat of vaporization
C_s = specific heat capacity of steam
T_2 = flue gas temperature
C_w = specific heat capacity of water
t_{m1} = feed temperature
G_c = dry material amount
C_m = specific heat capacity of dry material
t_{m2} = discharge temperature
$m_{1,2}$ = equivalent mass of particle
$I_{1,2}$ = equivalent rotational inertia of particle
s = radius of gyration
u_n = normal displacement of particle
u_s = tangential displacement of particle
θ = rotation angle of particle
F_n = normal force acting on particle
F_s = tangential force acting on particle
M = external torque
K_n = normal elasticity coefficient
K_s = tangential elasticity coefficient
c_n = normal damping coefficient
c_s = tangential damping coefficient
μ = friction coefficient between particles

1. Introduction

Drying drum is a device of heating, drying and transporting material. Due to its reliable operation, large operational flexibility, adaptability and strong processing power, drying drums are used in manufacturing process in a wide array of industries, including food, chemicals, metals, and buildings, etc.[1,2] In the drying process, energy saving and emission reduction are important technical indicators and major concerns to user companies. A good drying drum must lose as

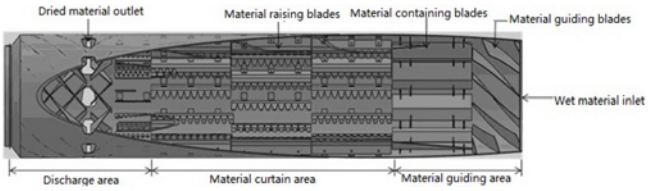

Fig. 1 Drying drum structure diagram

little energy as possible and complete the heat exchange between hot air and the aggregates in a short time. Hot air contacts the aggregates to vaporize the moisture, and the aggregates' temperature rises to the required value so it can achieve the ideal drying effect and thermal efficiency will be maximized.

The influencing factors of a drying drum's ability to dry mainly include the front inputting of the burner and the structural parameters of drying drum. The front inputting of a burner will influence the temperature field distribution in the drum, which directly determines the drum's overall drying outcome. The structural parameters of the drum will influence the drum's material curtain distribution characteristics, which determine the heat transfer effect between the aggregates and heat air current in the drum, thus influencing the drying outcomes of the drum.[3,4] Therefore, researching the drum's temperature field distribution characteristics and material curtain distribution characteristics is significant to improve the drying outcomes of rotary dryers.

For a long time, the research of drying drums was restricted to tests on the drying process and simple thermodynamic models. These studies cannot fully reveal the movement curve of the material in the drying drum or the temperature field distribution characteristics.[4]

With the development of computer technology, the computer can effectively model the temperature field distribution characteristics in the drying drum and the movement condition of the aggregate. This paper establishes a discrete element method (DEM) simulation model, researches the impact of drum structural parameters on the material curtain distribution by DEM, and studies the impact of the burner flame shape parameters on temperature field distribution in the drum based on fluid simulation analysis. The optimal design for a drying drum was achieved by comparing simulation and test results. The research results have great instructive significance in optimizing the parameters of drying drums and improving the drying outcomes of the drums.[5-8]

2. The Composition of a Drying Drum

The main body of a drying drum is a slightly tilted or horizontal cylinder that can rotate around its axis. Moist materials are fed into one side of the drum. When they move in the drum, they are dried by contact with a hot air current and heating wall. This paper presents a drying drum used in dry mortar mixing plants. Its design yield is 5t/h. Fig. 1 is a drum structure diagram.

In this drum, the moist materials and heating medium flows are parallel; therefore, the material containing blades that are designed to ensure that the blades can wrap materials in the material guiding area and materials will not drop into the material guiding area and affect the heat air current. Moist materials that need heating and drying are fed into one side of the drum and transported to the material raising blades by the material guiding blades and the material containing blades. The materials are raised and thrown by the material raising blades to form the material curtain. The formed material curtain fully contacts the heat air current to achieve heat exchange and dry the materials. The dried materials flow out from the material outlet, and the whole drying process is finished.

Table1 Relevant parameters of drying drum

Index	Value
yield of the drying drum G_1	5 t/h
water content of initial material W_1	5%
water content of product W_2	0.5%
specific heat capacity of dry material C_m	0.92 KJ/(kg·°C)
latent heat of stream q	2490 KJ/kg
stream temperature T_1	800°C
flue gas temperature T_2	104.5°C
feed temperature t_{m1}	20°C
discharge temperature t_{m2}	95°C

3. Research of the Temperature Field Distribution Characteristics in the Drying Drum

3.1 Material balance calculation of drying drum

Table 1 lists the parameters required of drying drum. After determining the design task of drying drum, amount of the liquid that need removing, drying medium consumption and the heat consumption were evaluated by making material balance calculation and heat balance calculation. Material balance is the basis of heat balance.[2]

The yield of the drying drum G_1 was calculated using Eq. (1).

$$G_1 = 5t/h = 5000kg/h = 1.389kg/s \quad (1)$$

The moisture content of dry basis C is related to wet basis W using Eqs. (2)~(3).

$$C_1 = W_1/(1-W_1) \quad (2)$$

$$C_2 = W_2/(1-W_2) \quad (3)$$

where C_1, C_2, W_1, and W_2 denote the moisture content of dry basis of initial material and product, and water content of initial material and product, respectively.

The calculation shows that C_1 = 0.0526, and C_2 = 0.0050.

The amount of dry material G_c, feed rate of sands G_0, and rate of evaporation W were calculated using Eqs. (4)-(5).

$$G_c = G_1 \cdot (1-W_2) \quad (4)$$

$$G_0 = G_c/(1-W_1) \quad (5)$$

$$W = G_c/(C_1-C_2) \quad (6)$$

The calculation shows that G_c = 1.382 kg/s, G_0 = 1.41 kg/s, and W = 0.0658 kg/s.

3.2 Heat balance calculation of drying drum

Drying is the process of using physical way to transfer heat to materials containing water. The heat is considered as latent heat, which removes the water.

During the process of drying materials in the drying drum, the heat consumption are mainly for latent heat of vaporization, heat of heating material, and thermal energy loss through system.[2]

When the yield of the drying drum is 5t/h, the heat quantity of evaporating water in wet material Q_1, heat quantity of heating materials Q_2, and thermal energy loss through system Q_3 were calculated using Eqs. (7)-(9).

$$Q_1 = W(q + C_s T_2 - C_w t_{m1}) \tag{7}$$

$$Q_2 = G_c \cdot C_m (t_{m2} - t_{m1}) \tag{8}$$

$$Q_3 = (Q_1 + Q_2) \times 15\% \tag{9}$$

where W, q, C_s, T_2, C_w, t_{m1}, G_c, C_m, and t_{m2} denote the rate of evaporation, latent heat of vaporization, specific heat capacity of steam, flue gas temperature, specific heat capacity of water, feed temperature, dry material amount, specific heat capacity of dry material, and discharge temperature, respectively.

The calculation shows that Q_1 = 171.27 kj/s, Q_2 = 95.36 kj/s, and Q_3 = 22.62 kj/s.

The total heat required Q was calculated using Eq. (10).

$$Q = Q_1 + Q_2 + Q_3 = 289.25 KJ/s \tag{10}$$

3.3 Simulation model of temperature field distribution

The temperature field distribution characteristics in a rotary dryer have a great influence on the drying outcomes. In order to improve the heat exchange between the hot air and the aggregates, the rotary dryer uses a burner. The burner flame dives into the drum directly and passes heat to the drum through flame radiation. The heat generated by the flame radiation forms a hot air current in the drum, which fully contacts and exchanges heat with the aggregates, and then the aggregate particles are heated and dried.

We used Fluent software which is based on finite volume method to simulate the temperature field in the drying drum. The finite volume method is a discretization method which is well suited for the numerical simulation of various types of conservation laws. Some of the important features of the finite volume method are similar to those of the finite element method. It may be used on arbitrary geometries, using structured or unstructured meshes, and it leads to robust schemes. An additional feature is the local conservativity of the numerical fluxes, that is the numerical flux is conserved from one discretization cell to its neighbor. The finite volume method is locally conservative because it is based on a “balance approach: a local balance is written on each discretization cell which is often called “control volume; by the divergence formula, an integral formulation of the fluxes over the boundary of the control volume is then obtained. The fluxes on the boundary are discretized with respect to the discrete unknowns.[9]

A 3D solid model of the drying drum was built and imported into pre-processing software. As shown in Fig. 2, the model is meshed into tetrahedral meshes, initialized and output to a grid file.[10,11]

Fig. 2 Drying drum mesh model

We built the solving model, set the fluid jet, defined the physical properties of the fluid domain and set the boundary conditions for the simulating calculations, using the fluent thermal radiation model (Rosseland model) to iteratively calculate the drying drum temperature field distribution. After 255 iteration steps, the results converged.[12]

According to practical case, the physical parameters of air were hypothesized and set as follows: Material Type (fluid), Density (1.225 kg/m^3), Specific Heat (1006.43 j/kgk), Thermal Conductivity (0.0242 w/mk), and Viscosity (1.7894^{-05} kg/ms).

For drying drum, the wall thickness was 6mm, so it could control the heat loss effectively and make the heat loss be only a very small portion of total heat. Therefore, we assumed that the drying drum was adiabatic and heat flux was 0 w/m^2. The drum wall temperature we measured was 800^{o}C. There were many factors that influenced heat transfer coefficient. After consulting documents and simulating many times, we determined heat transfer coefficient of air to be 10w/m^{2}k. Free stream temperature was the ambient air temperature, measuring 26.85. The drum wall was not the heat source, so heat generation rate was 0 w/m^3.

Therefore, the thermal boundary conditions of drying drum were as follows: Heat Flux (0 w/m^2), Temperature (800^{o}C), Heat Transfer Coefficient (10 w/m^{2}k), Free Stream Temperature (26.85), Wall Thickness (6 mm), Heat Generation Rate (0 w/m^3).

3.4 Affection of flame geometric parameters on drum temperature field distribution characteristics

The flame geometric features were obtained using the burning test of the burner. The flame length is 1100 mm, the maximum diameter is 280 mm, the distance between the largest diameter and the burner outlet is 320 mm, the flame diameter at the burner outlet is 160 mm and the outer flame temperature generated by the burner is 800^{o}C.

In order to access the validity of the simulation, the flame model was built according to obtained geometric features to simulate the temperature field distribution in drying drum, and then the distribution curve was obtained. In the same condition, we used burner to heat drying drum, the temperature field distribution in drying drum was measured using thermal infrared imager in field test. We can get comparison results in Fig. 3. It shows that simulation result and test result are basically identical. The temperature in drying drum decreases along the axial direction. The test result is slightly lower than simulation result, because the test was influence by environment to some extent and the drying drum lost some heat. Above all, simulation parameters are comparatively rational, and simulation results can basically reflect temperature field distribution in drying drum.

We changed the burner flame lengths to 600, 1100 and 1600 mm.

The temperature field distribution situation in a rotary dryer was simulated. Table 2 shows the flame characteristic parameters used in

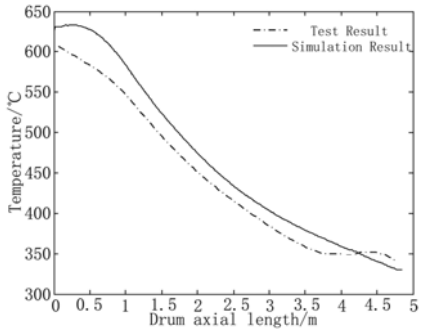

Fig. 3 Temperature field distributions curves of test and simulation

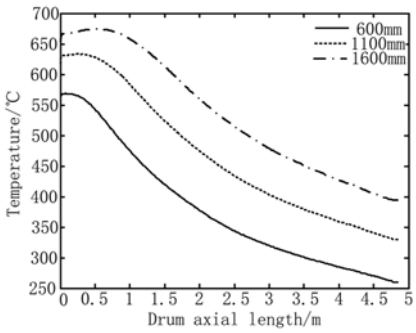

Fig. 5 Temperature distribution curves under different flame lengths

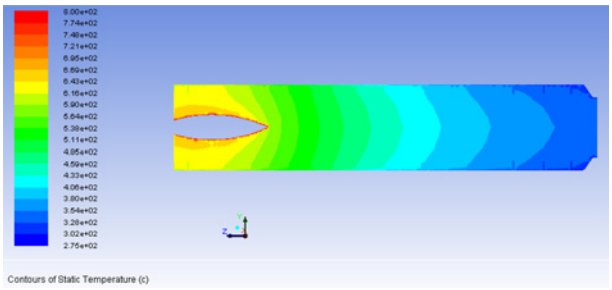

Fig. 4 Temperature field distribution in drying drum under the flame length of 1100 mm

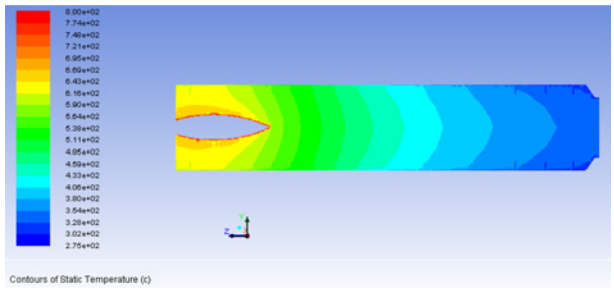

Fig. 6 Temperature field distribution in the drying drum under a flame diameter of 280 mm

Table 2 Flame characteristic parameters under different lengths

Index	Flame length (mm)	Flame maximum diameter (mm)	Outer flame temperature (°C)
1	600	280	800
2	1100	280	800
3	1600	280	800

Table 3 Flame characteristic parameters under different diameters

Index	Flame length (mm)	Flame maximum diameter (mm)	Outer flame temperature (°C)
1	1100	160	800
2	1100	280	800
3	1100	400	800

the simulation.

The models are built according to the flame geometric parameters shown in Table 2. After they were meshed, the grid files were imported using Fluent software, and the temperature field distribution in the rotary dryer was simulated. The results are shown in Fig. 4.

After analyzing and data processing the simulation results, we can get the distribution curves under different flame lengths, as shown in Fig. 5.

Figs. 4 and 5 show that changes in flame length have a prominent effect on the temperature field distribution. A too-short flame length leads to lower temperature and influences the drying outcome, which is disadvantageous for improving drum-drying efficiency. If the temperature in the drum rises, the length of the high-temperature area will increase, the length of the flame will increase and the theoretical drying outcome of the drum will improve. But in actual production, a set of materials containing blades covering the flame area should be installed. The material containing blade has two functions: it ensures that the aggregates will not fall into the material guiding area, and it allows aggregates that turn into the drum to be wrapped in the material containing blades and form a layer of material on the drum wall with the drum rotations. This layer of material will absorb most of the heat radiated by the burner flame in the material guiding area, and the drum wall will be protected. Thus, increasing flame length results in an increase of the length of the material containing blades and a decrease of the effective length of the drum material current area. However, heating and drying aggregates mainly occurs in the drum material current area. Hence, an overlong flame leads to a decrease in the effective length of the drum material curtain and goes against drying efficiency.

We set the flame length to 1100mm and changed the burner flame maximum diameters to 160, 280 and 400mm and then made simulations of the temperature field distribution in the rotary dryer. The flame characteristic parameters used in the simulation are shown in Table 3.

The model is built according to the flame geometric parameters shown in Table 3. After they were meshed into tetrahedral meshes, the grid files were imported using Fluent software, and simulations of the temperature field distribution in the rotary dryer were carried out. The results are shown in Fig. 6.

After analyzing and data processing the simulation results, we obtained the distribution curves under different flame diameters, as shown in Fig. 7.

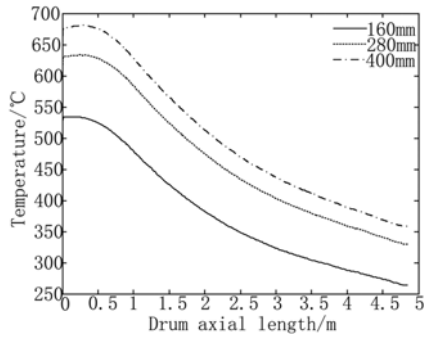

Fig. 7 Temperature distribution curves under different flame diameters

Figs. 6 and 7 show that the lengths of high-temperature areas are basically identical, even if the burner output flame diameters change. Therefore, the flame diameter has a small influence on the rotary dryer structure. When the burner output flame diameter is small, the temperature in the rotary dryer is low, and the drying effect of the aggregates is poor, which is disadvantageous for improving drum-drying efficiency. As the flame diameter increases, the temperature in the rotary dryer increases, the aggregates' drying outcome improves and the drying efficiency of rotary dryer improves. After analyzing the simulation results of the temperature field distribution in the rotary drum under different flame lengths and different flame diameters, we conclude that the burner flame length should match the rotary dryer structure. The flame length should not be too short and also should not surpass the installation site of the drum material containing blades. In the case of defining the flame length, a larger flame diameter is not necessarily better; one should rather choose a flame diameter suitable for the characteristics of the objects to dry and the drying goal. The flame diameter should be slightly larger than the ideal diameter meeting the drying requirement. In this design, the dryer not only can finish the drying task, but also reduce fuel consumption during the drying process and reduce production cost. In conclusion, the burner flame length should not be too short, and it should not surpass the installation site of the drum material containing blades. The flame diameter should be slightly larger than the ideal diameter meeting the drying requirement.

3.5 Experimental comparison of temperature field distribution

The drying drum experimental prototype was manufactured based on the design size of a ratio of 1:1. When making the drum run in normal conditions, design yield was 5 t/h. The output flame length was set at 1100 mm by adjusting the burner parameters. The flame maximum diameter was set at about 280 mm. The thermal imaging test was conducted on a drum using a Ti400 infrared thermal imager from Fluke Corporation. Fig. 8 shows the temperature distribution in normal operation.

Fig. 8(a) shows that because the drum is in a pre-heating process in the initial operating stage, the drum wall warming rate is slow. The material curtain formed by the aggregate particles is contaminated by flame radiation, so the aggregates' temperature rises faster and the aggregate drying process finishes. Therefore, the material curtain temperature in the drum is the highest, and the finished material

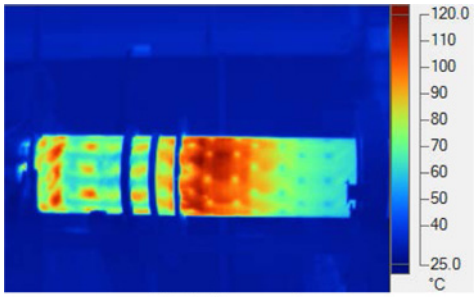

(a) Initial operating stage

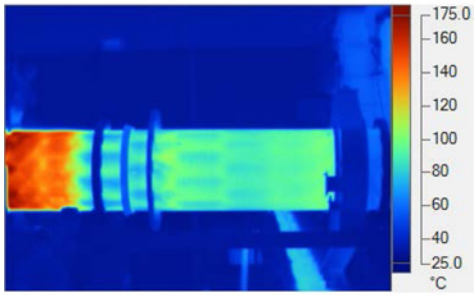

(b) Steady operating stage

Fig. 8 Thermal infrared spectrum of drying drum

temperature is about 103.2. Fig. 8(b) shows that, after the pre-heating process when the drum reaches a steady state, the drum wall is influenced by flame radiation. As the temperature rises, the drum reaches a steady state. The distribution of temperatures is a gradient distribution along the rotational center axis direction in the drying drum. The measured temperature distribution in the drying drum is basically identical to the simulation results above: the temperature of the drum nose close to the flame is higher; temperatures in the drum decreased along the rotational center axis direction the finished material's temperature is 93.4°C; and the drying effect meets the requirements.

4. Research on the material curtain distribution characteristics in a drying drum

The material curtain distribution characteristics in a rotary dryer determine the heat-exchange efficiency between aggregates and hot air current, which can be a big factor affecting drying outcomes. Researching the motions of aggregate particles in the drum and optimizing the drum structure can make the material curtain more uniform. A uniform material curtain allows the aggregate particles and hot air in the drum fully contacted each other and avoids hot air dissipation caused by the material curtain wind tunnel. All of this improves the drum drying efficiency.

4.1 The particle model of DEM

The discrete element method was used to study the material curtain distribution in a drying drum. DEM is a numerical method used to compute the stresses and displacements in a volume containing a large number of particles. The granular material is modeled as an assembly of rigid particles and the interaction between each particle is explicitly considered. The contact forces are calculated based on interaction

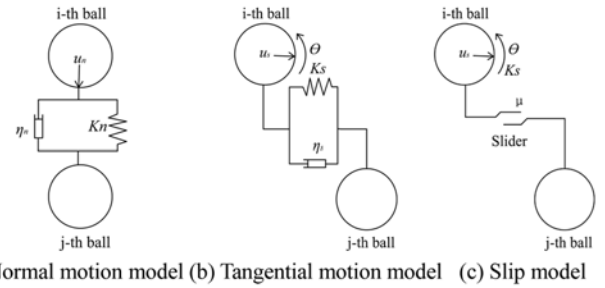

(a)Normal motion model (b) Tangential motion model (c) Slip model

Fig. 9 The motion models between particles

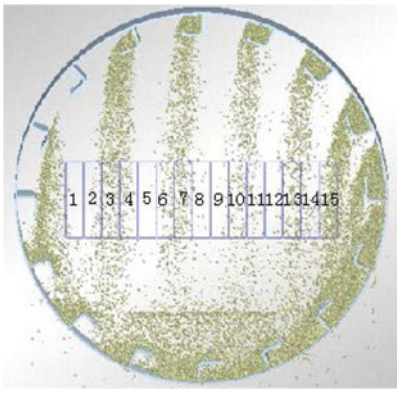

Fig. 10 Data statistics area division

forces between particles in every moment during the process. Then the motion parameters of elements are calculated by applying Newton's laws of motion. After repeated calculation, the movements of particles can be predicted.

In our study, the hard sphere model was used to describe inter-particle collisions. In DEM, the motions of particles are considered to be mutual independent. Only if the particles collide with each other will they interact at their contact point. In DEM, the particle model employs vibration equations to calculate force and displacement between particles, and between particle and boundary.[13] The normal motion model and tangential motion model between particles are shown in Fig. 9(a)-(b). The slip model between particles is shown in Fig. 9(c).

After resolving vibratory motion of particle collision, we obtained the equation of normal motion:

$$m_{1,2}d^2u_n/dt^2+c_n du_n/dt+K_n u_n = F_n \tag{11}$$

Tangential motion manifests as tangential motion and rolling:

$$m_{1,2}d^2u_s/dt^2+c_s du_s/dt+K_s u_s = F_s \tag{12}$$

$$I_{1,2}d^2\theta/dt^2+(c_s du_s/dt+K_s u_s)s = M \tag{13}$$

$m_{1,2}$, $I_{1,2}$, s, u_n, u_s, θ, F_n, F_s, M, K_n, K_s, c_n, and c_s denote the equivalent mass of particle, equivalent rotational inertia of particle, radius of gyration, normal displacement of particle, tangential displacement of particle, rotation angle of particle, normal force acting on particle, tangential force acting on particle, external torque, normal elasticity coefficient, tangential elasticity coefficient, normal damping coefficient, and tangential damping coefficient, respectively.

The rolling motion and tangential slippage of particles are influenced by friction between particles. The judgment condition of rolling motion and tangential slippage can be established based on slip model:

$$F_s = \mu K_n u_n \mathrm{sgn}[K_s(u_s+d\theta/2)] \tag{14}$$

μ denote friction coefficient between particles.[10]

4.2 Simulation experiment study of the material distribution characteristics

The following assumptions were made about the aggregates:

(1) The aggregates were spherical particles. The particle sizes were randomly distributed from 4 mm to 5 mm.

(2) The aggregates were absolutely dry, and the moisture content was not considered (moisture content of aggregate was 0%).

The 3D model of the drum was built based on the original proportions. The model was imported into EDEM software to be discrete element-analyzed and calculated, and then the simulation results of the drum material curtain distribution were obtained. The material curtain area was divided into 15 isopyknic units (Fig. 10), and the numbers of particles through each unit were counted. This reflects the uniformity of the material curtain distribution. If each unit has a roughly equal number of particles, it means that the material curtain distribution is relatively uniform, which is advantageous for the heat-exchange between particles and hot air, and the material curtain is of good quality. We changed the drum production parameters and material raising blade structure parameters in the material curtain area, conducted simulation on each parameter and analyzed the material curtain distribution formed by aggregate particles under each parameter.

The basic structure parameters of the drying drum were as follows: drum length (5 m), drum diameter (1 m), drum inclination (1.5), drum speed (8 rpm).

The drum production process parameters mainly include the drum inclination and drum speed. The effect of drum inclination mainly reflects the residence time of aggregates in the drum. The drum speed has an effect not only on the residence time of aggregates in the drum, but also on the uniformity of the material curtain. We chose different drum speeds (4, 6, 8, 10 and 12 rpm) and conducted simulation. The results are shown in Fig. 11.

Fig. 11 shows that drum speed determines the particles' initial velocity while leaving the blades. The higher the drum speed and the higher will be the particles' initial velocity, and then the whole material curtain area moves to the left side of the drum. A too high or too low drum speed will cause the material curtain to deviate to one side of the drum and not evenly cover the whole material curtain area. This is unfavorable for the heat-exchange between particles and hot air, and results in poor drum drying outcomes. According to the simulation results, the best drum speed should be between 6 and 8rpm.

The material raising blades used in the material curtain area are L type bending blades, as shown in Fig. 12. After being raised by the blades, the aggregate particles form a material curtain in two ways: some of the particles form a material curtain by dropping through gaps between the blade tooth spaces in the rising process, while others are

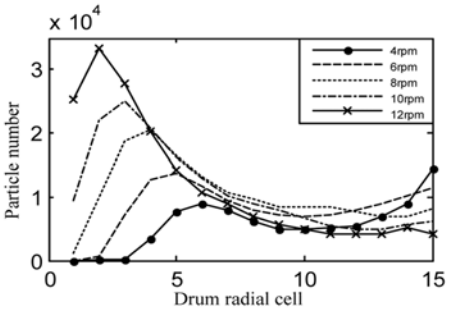

Fig. 11 Material curtain distribution in drum under different speeds

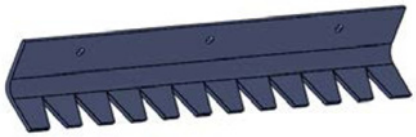

Fig. 12 Material raising blades structure diagram

Table 4 Structure parameters under different bending angles

Index	Bending angle/°	Tooth pitch /mm	Truss plate side length/mm
1	90	30	55
2	105	30	55
3	120	30	55
4	135	30	55
5	150	30	55

raised by the blades, turn a certain angle in the drum and then drop from the truss plate.

The drum speed was set to 8rpm; the drum inclination was set to 1.5. By changing the material raising blade (Fig. 12) structure parameters, the drum was simulation analyzed, and we can see how the blade structure parameters influence the material curtain formed in the drum runtime. Structure parameters include the blade bending angle, blade tooth pitch and truss plate side length. Table 4-6 list the specific blade structure parameters.

The blade parameters were set according to Table 4. The material curtain distributions in the drum with different material raising blade bending angles (90, 105, 120, 135, and 150) were simulation analyzed. The results are shown in Fig. 13.

Fig. 13 shows that changing bending angles directly influence the blanking position. If the bending angle is too large, the material curtain formed in the drum will be concentrated in the right side of the drum, the material curtain will be uniform and the wind tunnel phenomenon will be obvious. As the bending angle decreases, the material curtain moves to the left side of the drum, the material curtain becomes more uniform and the quality improves. However, if the bending angle is too small, the blades' raising skill will be affected. In that case, although the material curtain distribution is relatively uniform, the material curtain density will decrease, the drum thermal efficiency will decrease and the drum drying outcome will be influenced. Therefore, analysis of the simulation results suggests that a proper material raising blade

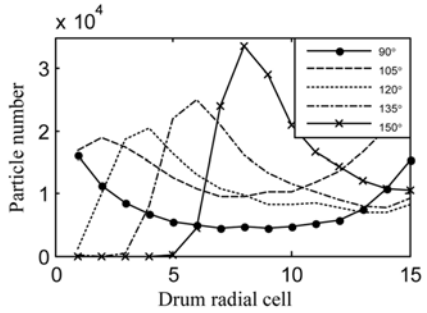

Fig. 13 Material curtain distributions under different bending angles

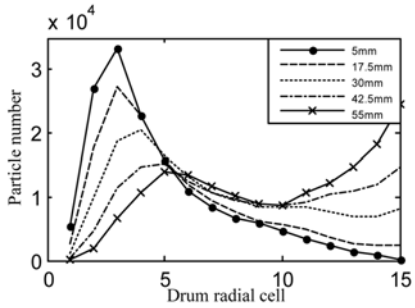

Fig. 14 Material curtain distributions under different tooth pitches

Table 5 Structure parameters under different tooth pitches

Index	Bending angle/°	Tooth pitch/mm	Truss plate side length/mm
1	120	5	55
2	120	17.5	55
3	120	30	55
4	120	42.5	55
5	120	55	55

bending angle is between 105 to 120.

The blade parameters were set according to Table 5. The material curtain distribution in the drum with different material raising blade tooth pitches (5, 17.5, 30, 42.5 and 55 mm) were simulation analyzed. The results are shown in Fig. 14.

Fig. 14 shows that changes in tooth pitch mostly affect the aggregates, which creep down between the tooth spaces. As the tooth pitch increases, the quantity of aggregates creeping down between the tooth spaces will increase, and a material curtain will form on the right side of the drum. If the tooth pitch is too big, the aggregates creeping down on the left side will decrease and cannot form a material curtain on the right side of the drum. If the tooth pitch is too small, the aggregates creeping down on the right side of the drum will decline, and a wind tunnel will appear on the left side. These both cause maldistribution of the material curtain, which adversely affects drum drying efficiency. Analysis of the simulation results suggests that an effective material raising blades tooth pitch is between 30 and 42.5 mm.

The blade parameters were set according to Table 6. The material curtain distributions in the drum with different material raising blade

Table 6 Structure parameters under different bending angles

Index	Bending angle/°	Tooth pitch/mm	Truss plate side length/mm
1	120	30	25
2	120	30	40
3	120	30	55
4	120	30	70
5	120	30	85

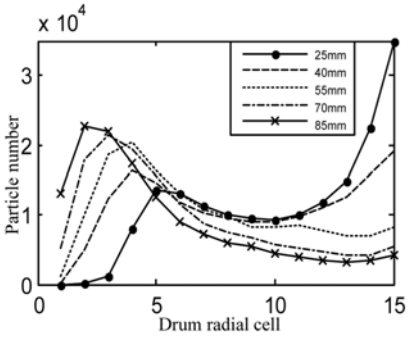

Fig. 15 Material curtain distributions under different truss plate side lengths

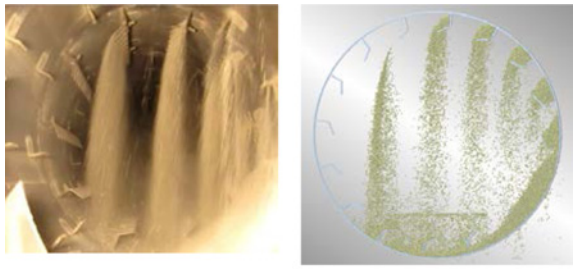

(a) The material curtain formed by optimized drum

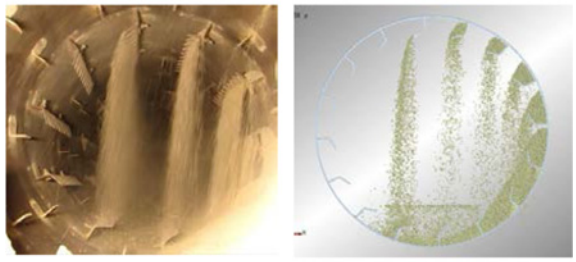

(b) The material curtain formed by un-optimized drum

Fig. 16 Results comparison diagram of prototype production test and discrete element simulation

truss plate side lengths (25, 40, 55, 70 and 85 mm) were simulation analyzed. The results are shown in Fig. 15.

Fig. 15 shows that the blade truss plate side length mainly affects the aggregates' spilling position. If the truss plate is too long, more aggregates will be raised to the left side of the drum by the blade then be dropped down, and the wind tunnel will appear on the right side of the drum. If the truss plate is too short, aggregates will drop down on the right side of the drum, and the wind tunnel will appear on the left side of the drum. Both lead to maldistribution of the material curtain and poor drying quality. Therefore, after analyzing the simulation results, the best material raising blades truss plate side length is between 40 to 55 mm.

4.3 Drying drum material curtain distribution test

We used the drying drum experimental prototype to conduct a drum material distribution test. The equipment is huge and requires big one-shot investments, so it is difficult to assemble and disassemble. Therefore, the experimental prototype cannot simulate all the parameters described above. We choose parameters that formed a high quality material curtain to do the validation test. The parameters of experimental prototype were as follows: drum speed (8 rpm), drum inclination (1.5), blade bending angle (120), truss plate side length (55 mm), tooth pitch (30 mm).

The production experiment was conducted according to the parameters above, and the drum production process was simulation analyzed using the same parameters. The results of the test and simulation are shown in Fig. 16(a).

As we can see in Fig. 16(a), the test result is consistent with the simulation result. The material curtain formation position and range are also the same. This indicates that the simulation results are reliable, so we can get optimized parameters for the drying drum system from simulations. We can also compare the optimized curtain with the material curtain formed by an un-optimized drum, which has been used in dry mortar mixing plants for a long time (Fig. 16(b)). It is obvious that the optimized drum is much more uniform. We can apply optimized parameters to experiment, and the experiment result can improve the simulation, so they will accelerate each other. They both serve actual production by reducing the cost of development and improving the drying outcome of drying drums.

5. Conclusions

This paper adopts fluid calculation software to simulate the temperature field distribution characteristics of a drying drum. A thermal infrared imager tests the actual temperature field distribution of a drying drum. The results showed that the simulation results are basically consistent with the test results; the drying drum temperature field simulation is accurate. Simulation analysis was carried out for the motion of aggregate particles and the distribution characteristics of the material curtain by DEM. The material curtain distribution characteristics of the prototype were site tested, and the results show that there is good agreement between the actual material curtain distribution characteristics and the simulation results. The optimized structural parameters and production parameters of a drying drum were obtained by DEM and fluid calculation simulation. The drying drum's optimum parameter design was achieved by an established multiphase flow simulation model. This drying drum will be more energy-efficient and environmentally friendly.

ACKNOWLEDGEMENT

This work was financially supported by the special project of

National and International Scientific and Technological Cooperation (2015DFA710402), major project foundation of science and technology in Fujian Province (2012H6014, 2014H6017) and Subsidized Project for Cultivating Postgraduates' Innovative Ability in Scientific Research of Huaqiao University.

REFERENCES

1. Shi, Y.-C. and Chai, B.-Y., "Present Situation and Development Tendency of Chinese Drying Technology," Drying Technology & Equipment, Vol. 4, No. 3, pp. 122-130, 2006.
2. Jin G., "Drying Equipment," Chemical Industry Press, p. 1, 2002. (In Chinese)
3. Wardjiman, C. and Rhodes, M., "Heat Transfer in a Particle Curtain Falling through a Horizontally-Flowing Gas Stream," Powder Technology, Vol. 191, No. 3, pp. 247-253, 2009.
4. Li, H., Kong, D., and Wang, P., "Numerical Simulation of Inner Flow Field and Heat-Transfer Process for Drying Drum," Journal of Engineering Machinery, Construction Machinery and Equipment, Vol. 42, No. 6, pp. 20-23, 2011. (In Chinese)
5. Tianjin, Y., Di, Y., Cheng, Y., and Yang, B., "Numerical Simulation of Temperature Field of Renewable Asphalt Mixing and Drying Drum," Journal of Construction Machinery Technology, Vol. 5, No. 3, pp. 267-271, 2007. (In Chinese)
6. Wardjiman, C., Lee, A., Sheehan, M., and Rhodes, M., "Behaviour of a Curtain of Particles Falling through a Horizontally-Flowing Gas Stream," Powder Technology, Vol. 188, No. 2, pp. 110-118, 2008.
7. Peinado, D., De Vega, M., García-Hernando, N., and Marugán-Cruz, C., "Energy and Exergy Analysis in an Asphalt Plant's Rotary Dryer," Applied Thermal Engineering, Vol. 31, No. 6-7, pp. 1039-1049, 2011.
8. Hobbs, A., "Simulation of an Aggregate Dryer using Coupled CFD and Dem Methods," International Journal of Computational Fluid Dynamics, Vol. 23, No. 2, pp. 199-207, 2009.
9. Eymard, R., Gallouët, T., and Herbin, R., "Finite Volume Methods," Handbook of Numerical Analysis, Vol. 7, pp. 713-1018, 2000.
10. Hu, G., "Analysis and Simulation of Granular by Discrete Element Method Using EDEM," Wuhan University of Technology Press, pp. 178-179, 2010. (In Chinese)
11. Geng, F., Xu, D., Yuan, Z., Wang, H., and Li, Bin., "Three Dimensional Numerical Simulation of Mixing Characteristics of Slender Particles in Rotary Dryer," Journal of Southeast University (Natural Science Edition), Vol. 38, No. 1, pp. 116-122, 2008. (In Chinese)
12. Kim, S., Kim, T., Lee, G.-B., Park, Y.-J., and Cho, S. W., "Parametric Numerical Study for Energy Savings in Industrial Drying Process," Int. J. Precis. Eng. Manuf., Vol. 15, No. 3, pp. 513-518, 2014.
13. Cleary, P. W., "Industrial Particle Flow Modelling using Discrete Element Method," Engineering Computations, Vol. 26, No. 6, pp. 698-743, 2009.